ACS APPLIED MATERIALS & INTERFACES

Research Article

www.acsami.org

Drug Release from pH-Sensitive Polymeric Micelles with Different Drug Distributions: Insight from Coarse-Grained Simulations

Shu Yu Nie, Wen Jing Lin, Na Yao, Xin Dong Guo,* and Li Juan Zhang*

School of Chemistry and Chemical Engineering, South China University of Technology, Guangzhou 510640, P. R. China

Supporting Information

ABSTRACT: How to control the release of drugs from pH-sensitive polymeric micelles is an issue of common concern, which is important to the effectiveness of the micelles. The components and properties of polymers can notably influence the drug distributions inside micelles which is a key factor that affects the drug release from the micelles. In this work, the dissipative particle dynamics simulation method is first used to study the structural transformation of micelles during the protonation process and the drug release process from micelles with different drug distributions. And then the effects of polymer structures, including different lengths of hydrophilic blocks, pH-sensitive blocks and hydrophobic blocks, on drug release are also studied. In the end, several corresponding design principles of pH-sensitive polymers for drug delivery are proposed according to the simulation results. This work is in favor of establishing qualitative rules for the design and optimization of congener polymers for desired drug delivery, which is of great significance to provide a potential approach for the development of new multiblock pH-sensitive polymeric micelles.

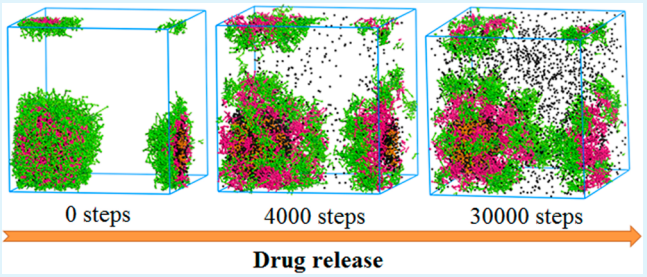

KEYWORDS: *dissipative particle dynamics simulation, pH-sensitive polymer, drug distribution, drug release, drug diffusion*

1. INTRODUCTION

In recent decades, the use of micelles prepared from amphiphilic polymers combining hydrophilic and hydrophobic blocks for drug delivery has attracted much attention.[1−3] It is well-known that micelles have an internal core composed of hydrophobic blocks as a loading space for hydrophobic drugs, whereas the hydrophilic blocks form a surrounding corona in an aqueous medium for the stabilization of micelles.[4,5] Polymers with the ability to encapsulate and release drugs in response to an acidic environment have become an exciting field of investigation.[6−8] The amphiphilic polymers modified with pH-sensitive groups can increase the selectivity for tumor cells and enhance intracellular drug delivery while reducing systemic toxicity and side effects.[9−12] In general, the weakly acidic/basic groups contained in the pH-sensitive polymers can release/accept protons according to the pH and ionic strength of the environment, leading to the distinct changes in the volume and solubility of polymers and thus monitor drug release. Oh et al. designed micelles having a self-assembled flower-like arrangement consisting of two hydrophobic blocks and a petal-like hydrophilic PEG block at physiological pH.[13] The doxorubicin (DOX) release from the micelles accelerated in response to tumor pH (<pH 7.0). Another pH-sensitive polymeric micelles synthesized by his group showed a pH-dependent micellar destabilization due to the concurrent ionization of the poly(L-histidine) and the rigidity of the poly(L-lactic acid) in the micellar core, resulting in the micelles triggering released DOX at pH 6.8 (i.e., cancer acidic pH) or pH 6.4 (i.e., endosomal pH).[14]

The effective application of polymeric micelles depends on their drug loading and release. The drug loading process has a great effect on the micelle loading capacity and efficiency of hydrophobic drugs. With regard to the drug release process from pH-sensitive polymeric micelles, once drug release is triggered in acidic environment, how can drug molecules pass through the polymeric matrix? This is the key issue determining whether drugs can take effect or not. For pH-sensitive polymeric micelles, the distribution of drugs in the micelles, the structure of pH-sensitive polymers, etc., can result in different drug release. However, direct experimental measurement to identify the effect of these factors on the drug release process is very difficult because of the space and time scale of the soft matter systems. Although there are plenty of experimental studies with regard to the size, drug loading capacity, and release concentration of pH-sensitive micelles, such as UV−vis spectroscopy, dynamic light scattering (DLS), scanning electron microscopy (SEM), and transmission electron microscopy (TEM), etc., detailed information from the microscopic and mesoscopic insight such as drug distribution in micelles, morphologies of micelles before and after protonation, drug release process as micelle swelling and so on are difficult to be characterized through present experimental technique and are seldom reported.

Received: June 19, 2014
Accepted: September 19, 2014
Published: September 19, 2014

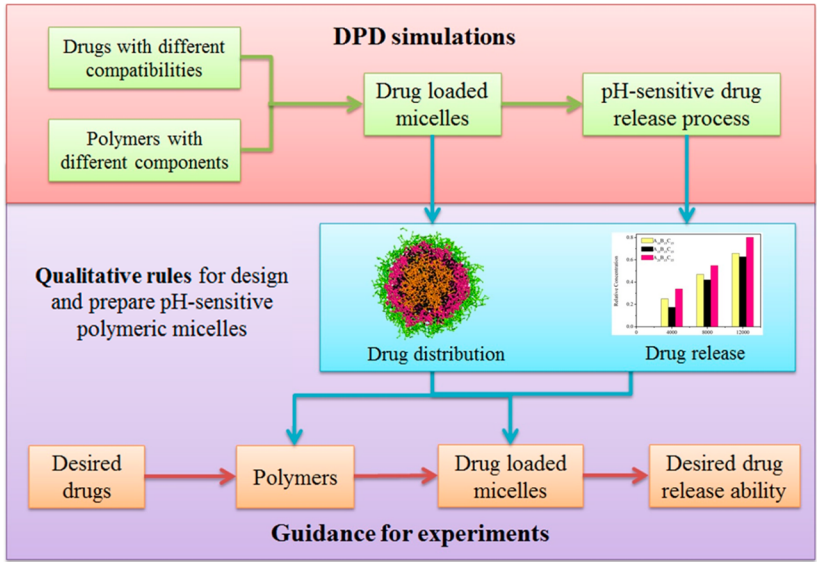

Figure 1. Research idea of this work.

In the absence of laboratory experiments, mesoscopic simulations offer a particularly useful method to explore the microphase separation of soft matter in complex systems for understanding and elucidating complex mechanisms such as drug release process from pH-sensitive micelles in an acidic condition.[15−21] Dissipative particle dynamics (DPD), proposed by Hoogerbrugge and Koelman in 1992 and revised by Español and Warren,[22,23] is one effective simulation method to investigate the phase behavior of complex fluids, providing a mesoscopic insight into the macro scale experimental system. The forces applied on DPD effectively stretch the characteristic time scale of the simulated system compared to the full atomistic and molecular dynamic simulation.[24−28] In addition, with the bead-and-spring model and by establishing a relationship between a simple function form of the conservative repulsion and the Flory−Huggins parameter theory, DPD method has been widely applied in simulations on structure and dynamics of soft matter.[29−34] Recently, Rodríguez-Hidalgo et al. studied the drug release mechanism on the polymeric vehicle P(ST-DVB) in an acid environment using DPD method.[35] Four transient stages were detected during the drug release: swelling of the microsphere, generation of pores, drug diffusion through the polymeric matrix and drug release toward the acid medium. However, few investigations on the factors influencing the drug release process from polymeric vehicles in polar environments have been reported. Therefore, a more thorough understanding of the drug release from pH-sensitive micelles will address many relevant issues to the drug delivery system.

As mentioned above, drug loading and release capacity of micelles are two main factors on the effective application of polymeric micelles. In our previous work, we have studied drug diffusion abilities into the core of micelles after the core−shell structure is formed.[36] The topological structure of drugs, the hydrophobic block length of the polymers, as well as the compatibility between the drug and the hydrophobic block showed profound effects on drug loading efficiencies and drug distributions inside micelles. Drug distribution inside micelles reflects miscibility and/or degree of interaction between a drug and polymer blocks, influences the performance of micelles with regard to drugs distribute, such as stability, drug-loading efficiency, drug release kinetics, etc. As to pH-sensitive micelles, drug distribution is also one of the key issues to determine the drug release capacity.[37] In general, pH-sensitive drug release abilities of micelles formed from polymers with identical structure are different due to various drug distributions. On the other hand, it is known that the structures of polymers can also influence the drug release from micelles. Therefore, to explore the complex relationship between the structure of pH-sensitive micelles with different block components and their release property with different drug distributions is of great importance.

In the present work, DPD simulations are carried out to study the relationship between the structures of pH-sensitive triblock polymers $A_lB_mC_n$ commonly used in experimental systems[38−41] and the drug release behaviors of the micelles. For clarity, the idea of this work is indicated as Figure 1. Three types of drug distributions inside micelles, designed by different compatibilities between the drugs and polymers, are prepared in DPD simulations: drugs distribute in (i) the pH-sensitive layer, (ii) both of the pH-sensitive layer and the core, (iii) the core of the micelles. To better understand the relationship, the structural transformation of the micelles during the protonation and the drug release process from the micelles with different drug distributions are first studied. Then the effects of the length of hydrophilic, pH-sensitive, and hydrophobic blocks on release process of drugs from the micelles after protonation are also studied. Finally, the guidance is proposed from the relationship between the structure of pH-sensitive polymers with different block components and the release property of micelles with different drug distributions based on the simulation results. The qualitative rules for the design of polymers with optimized block components based on the desired drug distributions could help design and prepare the pH-sensitive polymeric micelles with expected drug release ability, and provide a potential approach for the development of new pH-sensitive polymeric micelles.

2. SIMULATION METHOD

In the DPD method, a set of soft interacting particles are used to simulate a fluid system. Each particle represents a group of atoms or a volume of fluid that is large on the atomistic scale

but is still macroscopically small. All beads comply with Newton's equations of motion[42,43]

$$\frac{d\mathbf{r}_i}{dt} = \mathbf{v}_i,\ m_i\frac{d\mathbf{v}_i}{dt} = \mathbf{f}_i \quad (1)$$

Where $\mathbf{r}_i$, $\mathbf{v}_i$, m_i, and $\mathbf{f}_i$ denote the position vector, velocity, mass and total force on the particle i, respectively. For simplicity, the mass of all beads are set to 1 DPD unit. The force between each pair of beads is a sum of a conservative force ($\mathbf{F}_{ij}^{C}$), a dissipative force ($\mathbf{F}_{ij}^{D}$), and a random force ($\mathbf{F}_{ij}^{R}$)[44,45]

$$\mathbf{f}_i = \sum_{i\neq j}(\mathbf{F}_{ij}^{C} + \mathbf{F}_{ij}^{D} + \mathbf{F}_{ij}^{R}) \quad (2)$$

The conservation force for nonbonded particles is defined by soft repulsion. The dissipative force corresponding to a frictional force depends both on the position and relative velocities of the beads. The random force is a random interaction between bead i and its neighbor bead j. All forces vanish beyond a certain cutoff radius r_c, whose value is usually set to 1 unit of length in simulations. The three forces are given by the following formulas[46,47]

$$B_{ij}^{C} = \begin{cases} a_{ij}(1 - r_{ij})\hat{\mathbf{r}}_{ij} & (r_{ij} < 1) \\ 0 & (r_{ij} \geq 1) \end{cases} \quad (3)$$

$$\mathbf{F}_{ij}^{D} = -\frac{\sigma(\omega(r_{ij}))^2}{2kT}(\mathbf{v}_{ij}\cdot\hat{\mathbf{r}}_{ij})\hat{\mathbf{r}}_{ij} \quad (4)$$

$$\mathbf{F}_{ij}^{R} = \frac{\sigma\omega(r_{ij})\hat{\mathbf{r}}_{ij}\zeta}{\sqrt{\delta_t}} \quad (5)$$

where a_{ij} is the strength of the repulsive interaction and depends on the species of particles i and j, $\mathbf{r}_{ij} = \mathbf{r}_i - \mathbf{r}_j$, $r_{ij} = |\mathbf{r}_{ij}|$, $\hat{\mathbf{r}}_{ij} = \mathbf{r}_{ij}/|\mathbf{r}_{ij}|$, $\mathbf{v}_{ij} = \mathbf{v}_i - \mathbf{v}_j$, σ is the noise strength, ζ denotes a randomly fluctuating variable with zero mean and unit variance, δ_t is the time step of simulation, k is the Boltzmann constant, T is the absolute temperature. kT is considered as one unit in the simulations. The r-dependent weight function $\omega(r) = (1 - r)$ for $r < 1$ and $\omega(r) = 0$ for $r > 1$. In addition, an extra spring force ($\mathbf{F}_{ij}^{S}$, $\mathbf{F}_{ij}^{S} = -C\mathbf{r}_{ij}$, where C is the spring constant.) is introduced to describe the constraint between the bonded particles in one molecule. In this work, the spring constant is set to 4, resulting in a slightly smaller distance for bonded particles than for nonbonded ones.[16,47]

The coarse-grained model of polymers is shown in Figure 2. The polymers studied in this work are pH-sensitive ABC triblock polymers, where A (green), B (purple), and C (brown) represent hydrophilic block, pH-sensitive block, and hydrophobic block, respectively (although the pH-sensitive block B is hydrophobic before protonation, it becomes much more hydrophilic after protonation). The coarse-grained models of the polymers are designed based on the structures of pH-sensitive polymers commonly used in experimental systems. The hydrophilic blocks are designed with short side chains (namely branched hydrophilic blocks) and distributes on the surface of the self-assembled micelles, providing a compact steric protective layer to maintain the stability of micelles during biological circulation.[40,48,49] For simplicity, the pH-sensitive triblock polymers $(A(A_4))_lB_mC_n$ are named as $A_lB_mC_n$ in the paper, where l, m, and n are the length of the hydrophilic, pH-sensitive, and hydrophobic block, respectively. The characteristics of beads (either hydrophobic or hydrophilic) result in the value of interaction parameters (see Table 1).

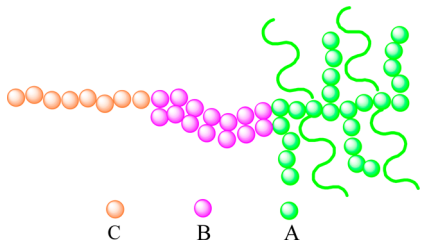

Figure 2. Coarse-grained model of pH-sensitive triblock polymer $(A(A_4))_lB_mC_n$.

Table 1. Interaction Parameters between Beads Used in the Simulations

a_{ij}	A	B	BH	C	D	W
A	25					
B	30	25				
BH	21		25			
C	40	30	100	25		
D	35	a^a	80	b^a	25	
W	26	35	11	55	45	25

[a]If drug molecules distribute in the pH-sensitive layer of the micelles, a = 25 and b = 30; in both the pH-sensitive layer and the core of the micelles: a = 28 and b = 27; in the core of the micelles: a = 30, b = 25.

Empirically, the interaction parameter between the hydrophilic blocks with water is close to 25 and the critical value of hydrophobicity is about 32.[50] Hence the interaction parameter between the hydrophobic blocks and water is set to a respectively high value and accordingly, the interaction parameter between the pH-sensitive blocks and water should be close to 32, showing a relatively weak hydrophobicity compared to the hydrophobic blocks. In the drug release process from pH-sensitive polymeric micelles, with the protonation of pH-sensitive block B, block B changes greatly to hydrophilic, resulting in the change of the interaction parameters between the pH-sensitive beads and other beads (the protonated B bead is donated by BH). Thus, in the drug release process of our simulations, the interaction parameters between the pH-sensitive bead (BH) and the hydrophobic beads (C and D) become larger, whereas those ones between BH and the hydrophilic beads (A and W) become smaller (the values are empirically smaller than 25). In this work, the pH-sensitive blocks are completely protonated during the drug release process. To investigate the effect of drug distribution on drug release, the pH-sensitive drug release processes of three types of drug distributions in micelles are analyzed and compared in the simulations, including drug molecules distribute in (i) the pH-sensitive layer, (ii) both of the pH-sensitive layer and the core, and (iii) the core of micelles. The micelles with different drug distributions are generated by introducing drugs having different interaction parameters with polymers that are determined through our preliminary tests. For simplicity, one drug molecule is set as one bead, denoted by D, which is in black color in our simulations. Each water bead is equivalent to one water molecule or a group of water molecules, denoted by W. In all the following figures, the water beads are concealed for clarity. Empirically, the volume fractions of the polymers, drugs and water are set to 10, 3,

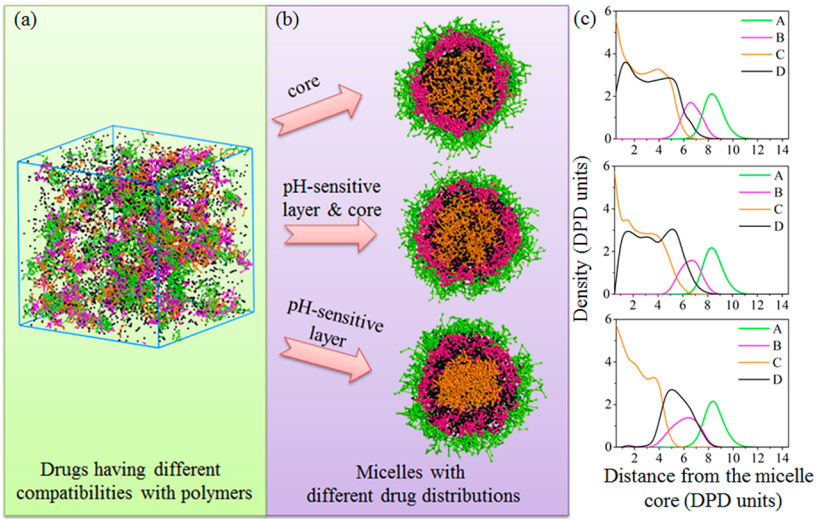

Figure 3. (a) Initial state of the simulation systems with components distributing randomly, (b) the $A_{10}B_{15}C_{15}$ micelles with different drug distributions before protonation and (c) their interfacial profiles of different beads.

and 87% in all DPD simulations for consistency, ensuring the micelles assembled in the systems are in stable and perfectly spherical structures.[51] Rectangular simulation boxes of 27 × 27 × 27 r_c^3 with periodic boundary conditions are used, the density of beads set as 3. The DPD simulations are performed for 300 000 time steps with an integration time step of 0.05 to achieve thermodynamic equilibrium and obtain drug-loaded micelles in neutral conditions. Then 10 000 time steps are used to analyze the drug release process from the micelles in protonation conditions. The simulations are performed by using the DPD program incorporated in the Materials Studio 5.5 software (Accelrys Inc.).

3. RESULTS AND DISCUSSION

As a starting point, the pH-sensitive polymers $A_lB_mC_n$ are placed in a watery environment with drug molecules homogeneously distributing in the solvents as shown in Figure 3a. Though DPD only possesses repulsive interaction, the collective repulsion can generate attraction between pairs of repulsive particles, thus aggregates can be organized.[52] Three types of drugs having different compatibilities with the polymers are used in this work to obtain three types of micelles with different drug distributions, as seen in Figure 3b. As for the drugs having good compatibility with the hydrophobic block C, they mainly distribute in the core of the micelles. For the drugs having good affinity with the pH-sensitive block B, they tend to locate in the middle layer. In the case that the affinities between the drugs and hydrophobic/pH-sensitive block are similar, the drugs can be observed in both the core and the middle layer. To show where the hydrophobic, hydrophilic, and drug components are, the interfacial profile of the micelles with different drug distributions (herein set $A_{10}B_{15}C_{15}$ micelles of an example) are also given, as shown in Figure 3c. The micelles with different drug distributions obtained in the watery system are served as the basis to explore the pH-sensitive drug release process in an acidic environment.

3.1. Structural Transformation and Drug Release from Micelles. To study the drug release mechanism from pH-sensitive polymeric micelles, we first discuss the structure transformation of the micelles after protonation. DPD simulations are employed in the micelles formed by $A_{10}B_{15}C_{15}$ with drugs distributing in the pH-sensitive layer, both pH-sensitive layer and core, and the core of the micelles during drug release process. Additionally, to further validate the changes on the morphology of micelles after protonation, the radius of gyration (R_g) of the hydrophilic and pH-sensitive blocks in different times are calculated in our DPD simulation. R_g is obtained from the mean square radius of gyration $\langle R_g^2 \rangle$ ($\langle R_g^2 \rangle = 1/N\sum_{i=1}^{n}(r_i - r_{cm})^2$, where N is the number of beads in a given polymer, r_i and r_{cm} are the position vector of each bead and the center of mass in the molecule, respectively),[50] which is defined as the root-mean-square distance of the beads in the micelles from their common center of mass, reflecting the extended degree of blocks in the space of the simulation system. Because the structural transformations of different micelles with different drug distributions are similar, thus the $A_{10}B_{15}C_{15}$ micelle with drug located in both the pH-sensitive layer and the core is used as an example to discuss the drug release process. Figure 4 shows the cross-section views of $A_{10}B_{15}C_{15}$ micelles in different simulation times during drug release process of the micelles (Figure 4a–c), and the radius of gyrations of the hydrophilic block A and pH-sensitive block B are calculated in the corresponding times (Figure 4d).

As shown in Figure 4, when the micelles are transferred to an acidic environment, the pH-sensitive blocks B become more hydrophilic after protonation, tending to stretch to the solvent (0–300 steps). In the initial phase of micelle swelling, the pH-sensitive blocks extend to the shell of the micelles generating a new shell with the original hydrophilic shell, which is denoted by A-B mixed shell (300–1000 steps). Accordingly, the R_g results of polymer blocks (Figure 4d), which characterize the structure differences of the micelles after protonation, show that the pH-sensitive blocks appear a sharp increase in R_g from 0 to 1000 steps. As the micelle swelling proceeds (1000–10000 steps), more water molecules diffuse into the micelles and the extension of pH-sensitive blocks reaches their maximum level, the growth of R_g becomes smaller because the blocks are close to a fully stretched state. As to the R_g results of hydrophilic blocks, the R_g values show a little decrease when the "A–B mixed shell–core" two layer structure forms, and a small growth of R_g values is observed during the transition to the "fireworks-like" three layer structure (which is named according

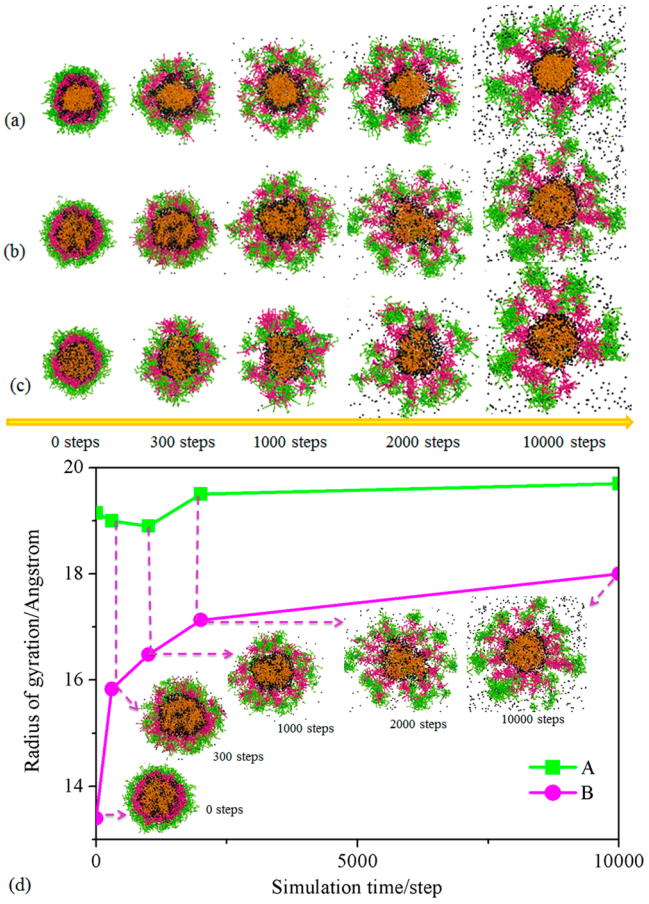

Figure 4. Cross section views of the micelles during drug release with different drug distributions: (a) the pH-sensitive layer, (b) both the pH-sensitive layer and the core, and (c) the core of the micelles. (d) Radius of gyration of block A and B of $A_{10}B_{15}C_{15}$ micelles in different simulation times.

to the structure, which looks like fireworks that the protonated chains stretch to the solvent surrounding the hydrophobic core) because the hydrophilic blocks recover fully stretched. The R_g results validate the changes on the morphology of the micelles after protonation. Due to the swelling of pH-sensitive blocks, the hydrophilic blocks also become more swelling and diffuse from the "A−B mixed shell" to the external space, forming a new third outer layer. In this phase the micelle generates many channels, which is denoted by a "fireworks-like" three-layer structure. The formation of channels in the "fireworks-like" micelles can facilitate the drug release from the micelles. We can know from this process that the "A−B mixed shell−core" two-layer structure micelle is the transition state to the "fireworks-like" three-layer structure. It should be noted that the rapid protonation followed by micelle swelling, which may not be that relevant to the practical situation, but it does not influence the transformation trend of the micelle structure and the qualitative comparison on the drug release of different micelles, which is supported by the comparison with our previous study in the swelling process of micelles when they are under different protonation levels.[51] On the whole, the transformation of the micelles loaded drugs with different affinities appears a similar trend: "shell−middle layer−core" three-layer structure → "A−B mixed shell−core" two layer structure → "fireworks-like" three layer structure. Figure 5 shows the schematic drawing of structural transformation of the pH-sensitive polymeric micelles at low pH conditions.

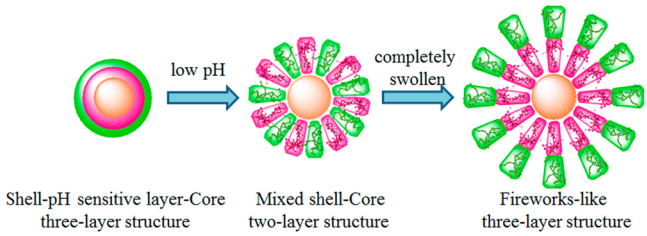

Figure 5. Schematic drawing of the structure transformation of the pH-sensitive polymeric micelles during micelle swelling.

In this section, we also explored the effect of drug distributions on the release processes of micelles. In the case drugs distribute in the pH-sensitive layer of the micelles (Figure 4a), a great number of drugs release accompanied by the stretch of the protonated pH-sensitive blocks. However, drugs do not release completely as the micelle transforms to the fireworks-like structure, and the drug release is still a successive and slow process. In the cross-section view of the micelles, a "sustained release area" can be observed, which refers to the drug layer surrounding the surface of the inner core. According to the simulation results, the drug release process from the pH-sensitive layer is speculated. On one hand, the outmost drugs of the "sustained release area" play a protective role to the ones that they cover. The outmost drugs release fast as they expose to the solvent while the ones protected by the outmost drugs stay in the micelles temporarily. As the diffusion of the outmost drugs, the ones that they cover become the outmost ones and act as the protective layer to the ones they surround. So the sustained release of drugs may achieve by the process of the replace of outmost drugs. On the other hand, the hydrophobicity of drugs leads to better compatibility with the hydrophobic core, which may avoid instant and complete release of drugs for a period of time.

As the drugs distribute in both of pH-sensitive layer and core of the micelles (Figure 4b), the early release of the micelles may be mainly attributed to the release of drugs companied by the extension of the pH-sensitive blocks. However, the drugs distribute in the pH-sensitive layer but cannot be completely released as soon as the protonated blocks stretch, which remain in the micelles temporarily and are released until the firework-like structure is formed through the increased channels generated in the micelles. This part of drugs may mainly contribute to the second phase of release. For other drug molecules located in the inner core of the micelles, their release needs to pass through three barriers: the polymeric matrix of the core, middle layer, and shell. Among these barriers, the resistance generated by the core is the main barrier due to the good compatibility between the drugs and the core, as well as the tense structure of the core even after protonation. Therefore, the drugs distribute in the core release quite slowly, achieving the sustained release of the micelles.

With regard to the drugs distributing in the core of the micelles (Figure 4c), by the phase that the "A−B mixed shell−core" two-layer structure is formed, the structure of the micelles is still in a relatively tense state, thus the release of drugs from the inner core is mainly promoted by diffusion. Therefore, in this phase the drugs need to pass through a relatively tense and complete polymeric matrix, showing a slow release rate. As the

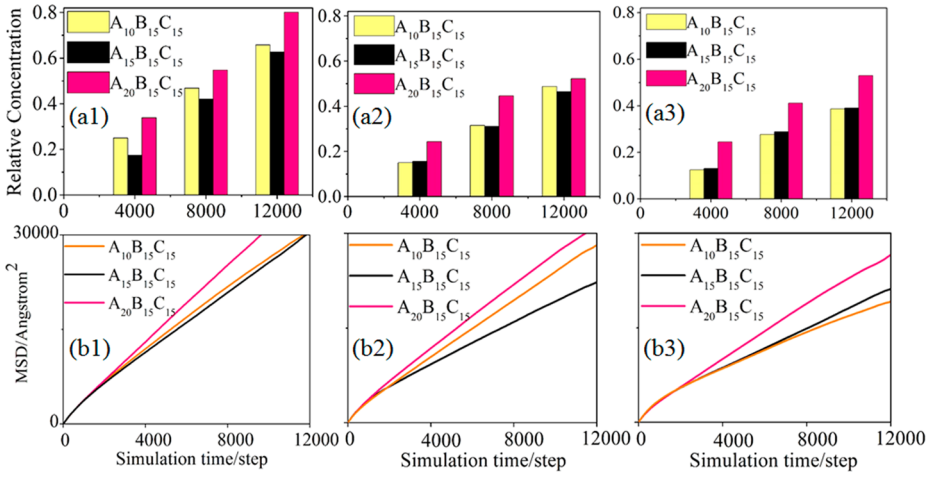

Figure 6. Relative concentrations and mean square displacements of the released drugs having different compatibilities with the micelles composing different lengths of A block: drugs distribute in (a1, b1) the pH-sensitive layer, (a2, b2) both the pH-sensitive layer and the core, and (a3, b3) the core.

simulation time increases, the extension level of the pH-sensitive block B increases, leading to larger channels generated among the blocks as well as increasing the exposed area of the core to solvent, which can decrease the resistance drugs need to overcome when release. Thus, more drugs being released are observed in the phase of fireworks-like structure. It should be noted that the drugs cannot be released completely because they need the degradation of hydrophobic blocks. The degradation of constituents in micelles is an important step in the release of drugs.[53] Besides, because of the hydrophobicity of drugs, the affinity between the drugs and the hydrophobic block of the micelles is better compared to water molecules. Therefore, complete drug release cannot be observed in the simulations.

3.2. Effect of Hydrophilic Block Length on Drug Release. Hydrophilic blocks play an important role in keeping the stability of micelles. Whether the hydrophilic blocks can affect the drug release of micelles and in what way they make influence on the drug release from micelles are investigated in this section. To investigate the effect of hydrophilic block length on drug release, three polymers $A_{10}B_{15}C_{15}$, $A_{15}B_{15}C_{15}$, and $A_{20}B_{15}C_{15}$ with different hydrophilic block lengths are used in this section.

On the basis of the transformation of the micellar structure during protonation, the drug release processes in the systems from micelles formed by $A_{10}B_{15}C_{15}$, $A_{15}B_{15}C_{15}$ and $A_{20}B_{15}C_{15}$ are analyzed. To reflect the drug release abilities during the release process, the relative concentrations of drugs (D beads) are obtained in the Mesocite module of Materials Studio 5.5 software by computing the ratios of D beads released into the water phase to all the D beads in the system at different simulation time. According to the relative concentration curves of the micelles and drugs, the curves of drugs show an obvious peak inside the micelle curves, which refer to the D beads remaining in the micelles, whereas the rest areas of the drug curves present the released D beads. Thus, the released D beads are able to be distinguished from the D beads which remain in micelles through the distribution of drugs reflected by this means. Moreover, to further study the effect of the blocks length on drug diffusion from the pH-sensitive micelles, we calculated the mean square displacements (MSD) of drugs in different simulation systems during the drug release process. MSD is the distance the beads move from their original position to the second moment of their distribution in a defined time span, defined as $\mathrm{MSD} = 1/N\sum_{i=1}^{N}|\mathbf{r}_i(t) - \mathbf{r}_i(0)|^2$, which is related to the diffusion coefficient ($F_D = (1/6N)\lim t_{t\to\infty}(\mathrm{d}/\mathrm{d}t)\sum_{i=1}^{N}|\mathbf{r}_i(t) - \mathbf{r}_i(0)|^2$), where $\mathbf{r}_i$ denotes the position vector of ith bead, N is the number of statistical beads. The MSD are also computed in the Mesocite module of Materials Studio 5.5 software. Herein, the MSD of drugs are used to analyze the diffusion behavior of the drugs during the release process. Notably, even though the MSD value of D beads is connected to the drug release, high MSD value is not always equal to fast drug release because the MSD value is a statistical outcome including the value of D beads have not released from the micelles but move inside the micelles. However, MSD results can reflect the resistance the drugs overcome when they move and help analyze in what way the lengths of blocks affect drug release process.

The relative concentrations of the released drugs from micelles formed by the polymers $A_{10}B_{15}C_{15}$, $A_{15}B_{15}C_{15}$, and $A_{20}B_{15}C_{15}$ at different simulation times are presented in Figure 6a, from which the changing trends of the concentrations of released drugs from micelles with different hydrophilic block lengths are shown. Compared to $A_{10}B_{15}C_{15}$, the drug release concentrations of the micelles formed by $A_{15}B_{15}C_{15}$ generally decrease or do not appear an obvious change, whereas for the micelles formed by $A_{20}B_{15}C_{15}$, the drug release concentrations show an outstanding increase. According to the morphologies of the micelles obtained in the simulations, the changing trends of the release concentrations are analyzed: The polymers with longer hydrophilic block A ($A_{15}B_{15}C_{15}$) can form micelles with stronger stability because of the thicker hydrophilic shell. Besides, the drugs need to pass through a thicker shell before release thus leading to a slower drug release, or a unapparent change when more drugs distribute in the core whose release rely on the degradation of the core. However, as the length of hydrophilic block further increases ($A_{20}B_{15}C_{15}$), more micelles are formed in the simulation because of the formation process of micelles. In initial phase, a small plenty of polymers form small aggregates, which will gradually collide and integrate into large aggregates and finally micelles are formed through stabilization. In the case, that the polymers with longer hydrophilic block, which leads to lower exposing extent of

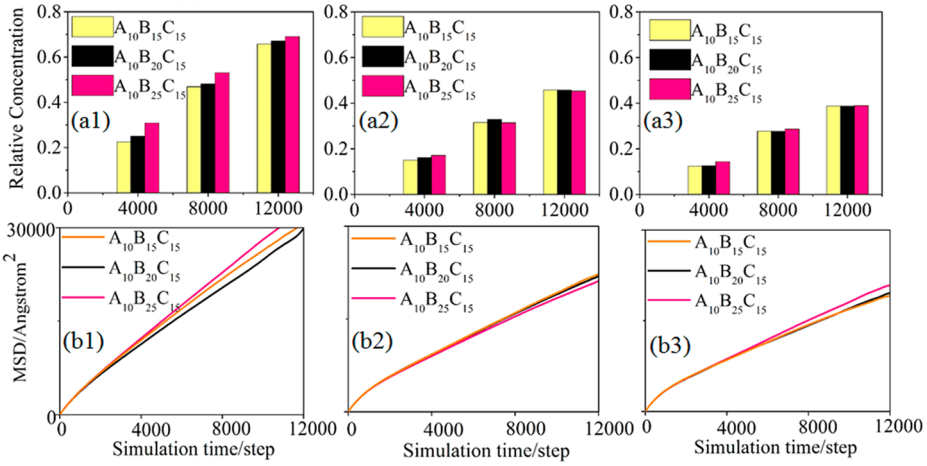

Figure 7. Relative concentrations and mean square displacements of the released drugs having different compatibilities with the micelles composing different lengths of B block: drugs distribute in (a1, b1) the pH-sensitive layer, (a2, b2) both of the pH-sensitive layer and the core and (a3, b3) the core.

the hydrophobic part of the aggregates, thus it is difficult for the aggregates to form into one large micelle even though through a long time collision and hence the number of the micelles increase as we observe (see the Supporting Information, Figure S1). Therefore, the micelles obtained in this case owning smaller core and sparse hydrophilic shells, thus the diffusion barrier of drug release becomes weaker and more drugs release in the same period of time. Additionally, as the number of micelles increases, the number of polymers in one micelle decreases, therefore the network generated among the polymers induces less space assistance to the drugs, which is in favor of the movement of the drugs. Besides, Figure 6a also shows that the changing trends of the concentrations of the released drugs with different distributions are similar that $A_{20}B_{15}C_{15}$ micelles show a highest release concentration no matter with drugs located in the pH-sensitive layer, both the pH-sensitive layer and the core, or the core.

The MSD curves of the released drugs from the micelles formed by the three polymers show in Figure 6b and the results of b1−b3 refer to the micelles with different drug distributions. The MSD curves show the diffusions of drugs from different parts of micelles are similar and the increase of length of hydrophilic block beyond a certain range ($A_{20}B_{15}C_{15}$) shows a remarkable influence on the diffusion of drugs. As the length of A block further increases to 20, the MSD curves of $A_{20}B_{15}C_{15}$ appear a rapid increase trend, indicating the movement of drugs becomes more active, which may also be due to the effect generated by the increased amount of micelles mentioned above that gives less space assistance to the drugs.

To sum up, no matter how the drug distributions inside the micelles are, the length of the hydrophilic block is in connection with the drug release, and different affinities between drugs and micelles show a similar changing trend of release. The shell of the micelles formed by the hydrophilic block not only maintains the stability of the micelles, but also has an outstanding effect on the drug release ability of the micelles. Therefore, when we design and prepare the drug-loaded micelles, the consideration of the overall influence of the hydrophilic block length, including its stability function and drug release effect to micelles, is of great importance.

3.3. Effect of pH-Sensitive Block Length on Drug Release. The pH-sensitive block is an important component of pH-sensitive micelles. To study the effect of pH-sensitive block length on drug release, we used three pH-sensitive polymers $A_{10}B_{15}C_{15}$, $A_{10}B_{20}C_{15}$,and $A_{10}B_{25}C_{15}$ with different lengths of pH-sensitive block in this section. The simulation parameters and the concentrations of components are in common with the above study except for the polymers used. The relative concentrations and MSD of drugs are also obtained at different simulation times (Figure 7).

In the case that the drugs distribute in the pH-sensitive layer of the micelles (Figure 7a1), the release of drugs is much faster than those of the other two cases (Figure 7a2, a3) because the relative concentration of released drugs is higher within the same period of simulation time. Accordingly, the MSD of drugs in Figure 7b1 are larger than those in Figure 7b2 and b3, and the MSD of $A_{10}B_{25}C_{15}$ are larger than those of $A_{10}B_{15}C_{15}$ and $A_{10}B_{20}C_{15}$ in Figure 7b1.

On the other hand, when drugs mainly distribute in the pH-sensitive layer of the micelles (Figure 7a1), the drug release shows a relatively remarkable increase when the length of B block increases in the initial phase at 4000 and 8000 steps compared to that at 12 000 steps, especially when B block increases to 25. This phenomenon may result from the fact that the extension trend of the pH-sensitive block is rather strong at the initial swelling process of micelles, the mechanically propelled effect (which is a kind of force generated by the stretch of protonated blocks that promotes the movement of drugs) acting on the drugs is most distinctive. Besides, when the drugs are mainly located in the pH-sensitive layer, longer pH-sensitive block leads to more drugs released through the stretch of protonated blocks. Furthermore, the strong hydrophilicity of the protonated blocks is in favor of the solvation of water molecules, which can enter the micelles easily and make the movement of drugs more active. However, the growths of the relative drug release concentration at 12 000 steps are not as remarkable as the ones at 4000 and 8000 steps. It may due to the fact that in the later phase of the drug release process, the micelles are almost completely swollen and the mechanically propelled effect generated by the stretch of pH-sensitive blocks acting on the drugs almost disappears. In this phase, the release of drugs is mainly through diffusion. Thus, it can be observed that the initial drug release rate is faster than that of the later

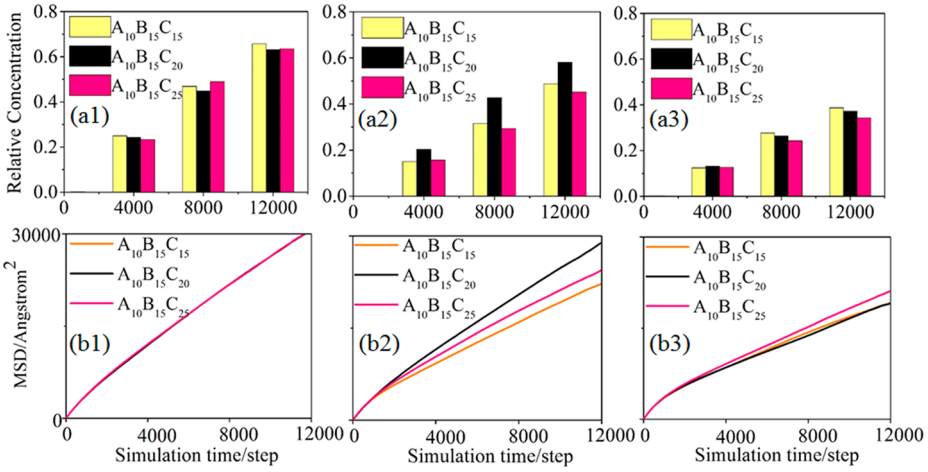

Figure 8. Relative concentrations and mean square displacements of the released drugs having different compatibilities with the micelles composing different lengths of C block: drugs distribute in (a1, b1) the pH-sensitive layer, (a2, b2) both the pH-sensitive layer and the core, and (a3, b3) the core.

phase and the pH-sensitive block shows a great influence on the initial drug release process.

With regard to the drugs distribute in both of the middle layer and the core, as well as mainly distribute in the core (Figure 7a2, a3), the increase in the pH-sensitive block does not show an obvious improvement to drug release. The reason may be that in these two cases of our simulations, the concentrations of drugs are not high enough to saturate the pH-sensitive layer, thus the mechanically propelled effect generated by the stretch of the pH-sensitive blocks acts on limited drug molecules, and a plenty of drugs located in the core are not affected by the stretch of the blocks. Hence, the length of the pH-sensitive block does not appear a significant influence on drug release and diffusion of these two cases in our simulations.

In conclusion, the pH-sensitive blocks improve the drug release ability of micelles because the mechanically propelled effect generated by the extension of the pH-sensitive blocks has a significant influence on the drug release. Besides, the effect of pH-sensitive blocks depends on the distribution of drugs, the promotion effect of pH-sensitive blocks enhances when more drugs distribute in the pH-sensitive layer. So when it comes to prepare drug loaded micelles, the compatibility between the drugs and the polymers should be put into the first place to decide the length of the pH-sensitive block. For instance, in the case that the release rate of the micelles is expected to be increased but the desired drugs has a better affinity with the hydrophobic block than the pH-sensitive block, to increase the length of the pH-sensitive block maybe not effective and other factors should be considered.

3.4. Effect of Hydrophobic Block Length on Drug Release. The hydrophobic block of polymers plays an important role in drug loading of micelles. However, is it true that the hydrophobic blocks have little influence on the drugs release of micelles? In this part, the effect of hydrophobic block on drug release of micelles is explored. The simulations are also performed on micelles with three types of drug distributions. The simulation parameters and the concentrations of components are in common with the above studies except for the polymers used. The pH-sensitive polymers with different lengths of hydrophobic blocks C are explored in this section, which are $A_{10}B_{15}C_{15}$, $A_{10}B_{15}C_{20}$ and $A_{10}B_{15}C_{25}$.

As seen from Figure 8a1, b1, the trend of released drug concentrations and the MSD curves of the micelles with different hydrophobic block lengths are not pronounced, indicating that the change in the length of the hydrophobic block has little influence on the drug release from the pH-sensitive layer of micelles.

By contrast, as to the drugs having similar affinity with the pH-sensitive and hydrophobic blocks (Figure 8a2), the drug release rate increases obviously as the hydrophobic block C becomes longer (from 15 to 20) interestingly. The reason is speculated as follows. As the previous section discussed, the transformation of micelles from the core−pH-sensitive layer−shell structure to fireworks-like structure generates many channels inside the micelles, resulting in the exposure of the core to water, allowing water molecules transfer to the micelles easily and thus accelerates the diffusion of drugs. Thus, the core formed by longer hydrophobic block provides larger exposed area to water after protonation when the length of block A and B are unchanged, the cross-section view of the micelles formed by $A_{10}B_{15}C_{15}$ and $A_{10}B_{15}C_{20}$ are shown in Figure 9. Also, the schematic drawing to explain the transformation in the structure of the micelles with longer hydrophobic block is shown in Figure 9. On the other hand, most drug molecules are located in the core of the micelles in this simulation system, particularly in the interface of the core and the middle layer. Therefore, larger exposed area with a great number of drugs is in favor of the drug release, which is in agreement with the MSD curves in Figure 8b2 that the curve of $A_{10}B_{15}C_{20}$ shows a sharp increase compared to $A_{10}B_{15}C_{15}$. However, it is shown that when the length of hydrophobic block C further increases (from 20 to 25) (Figure 8a2), the network formed among the hydrophobic blocks in the core may become more compact, in the meanwhile the surface area of the core increases, generating greater resistance to the diffusion of drugs. In this case, on one hand, the increase in the length of the hydrophobic blocks is in favor of the movement of the drugs distributing in the interface between the middle layer and the core. On another, it also strengthens the space resistance to the movement of the drugs loaded in the core. Thus, when it comes to prepare the micelles with drugs loading in both of the middle layer and the core, both of these effects should be taken into consideration.

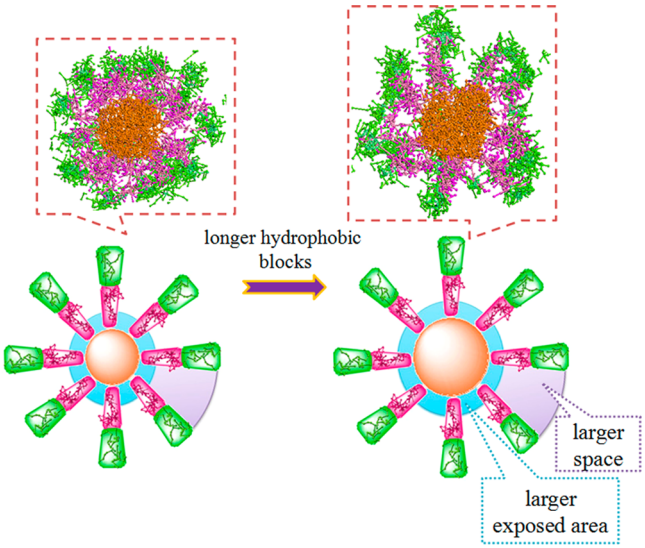

Figure 9. Schematic drawing of transformation in the structures of micelles with longer hydrophobic block.

As to the drugs mainly distribute in the inner core of the micelles (Figure 8a3), the MSD curves illustrate that drug diffusion is faster than those with shorter C blocks, which is due to the increasing surface area of the core, so the movement of drugs prompted by the water molecules. However, as mentioned before, faster drug diffusion does not always result in higher drug release rate, herein longer hydrophobic block also increases the release route of drugs, thus the drug release does not show a significant rise, or even appears a decline more often, as shown in Figure 8a3.

Overall, when we design the length of the hydrophobic blocks, the compatibility of the drugs and the polymers is a priority because different drug distributions in the micelles influence the drug release of the micelles with different lengths of hydrophobic block in distinct ways. Furthermore, the integral effect of the two opposing actions caused by the increase in the hydrophobic blocks should be well understood, and then the micelles owning desired drug release ability with certain length of the hydrophobic blocks could be prepared reasonably.

4. CONCLUSION

In this work, dissipative particle dynamics simulations are carried out to study the relationship between the structure of pH-sensitive triblock polymers and drug release behaviors from the micelles. The simulation results show that the "fireworks-like" three layer structure is of great importance to the drug release, and different drug distributions induce different drug release processes. Several design principles are proposed based on the simulation results: (i) The length of the hydrophilic block is in connection with the drug release and different drug distributions in micelles show a similar changing trend of the release. The length of the hydrophilic block needs to be decided on the overall consideration of its stability function and drug release effect on the micelles. (ii) The length of the pH-sensitive block has a profound influence on the drug release ability of the micelles, and when more drugs distribute in the pH-sensitive region, its promotion effect becomes stronger, thus the compatibility between the drugs and the micelle should come to the first place when design the length of pH-sensitive block. (iii) The drug release from micelles with different lengths of hydrophobic block is influenced in distinct ways with different drug distributions in the micelles, therefore the compatibility of the drug and the polymers should be considered in prior when determine the length. Moreover, the integral effect of the two opposing actions caused by the increase of hydrophobic blocks should be well managed. The design optimization strategies could help design and optimization of congener polymers for desired drug delivery, and might develop a potential approach for the design of new multiblock pH-sensitive polymeric micelles.

■ ASSOCIATED CONTENT

Supporting Information

Structures of micelles formed by $A_{20}B_{15}C_{15}$ in neutral and acidic pH. This material is available free of charge via the Internet at http://pubs.acs.org.

■ AUTHOR INFORMATION

Corresponding Authors

*E-mail: celjzh@scut.edu.cn. Telephone/Fax: +86-20-87112046.

*E-mail: cexdguo@scut.edu.cn. Telephone/Fax: +86-20-87112260.

Notes

The authors declare no competing financial interest.

■ ACKNOWLEDGMENTS

This work was financially supported by National Natural Science Foundation of China (21176090, 21206045), Team Project of Natural Science Foundation of Guangdong Province, China (S2011030001366), Specialized Research Fund for the Doctoral Program of Higher Education of China (20130172110009), and Fundamental Research Funds for the Central Universities, China (013ZP0010, 2013ZZ0059, 2014ZP0020).

■ REFERENCES

(1) Shen, Y.; Zhan, Y.; Tang, J.; Xu, P.; Johnson, P. A.; Radosz, M.; Van Kirk, E. A.; Murdoch, W. J. Multifunctioning pH-Responsive Nanoparticles from Hierarchical Self-Assembly of Polymer Brush for Cancer Drug Delivery. *AIChE J.* **2008**, *54*, 2979−2989.

(2) Sutton, D.; Nasongkla, N.; Blanco, E.; Gao, J. Functionalized Micellar Systems for Cancer Targeted Drug Delivery. *Pharm. Res.* **2007**, *24*, 1029−1046.

(3) Chen, D.; Song, P.; Jiang, F.; Meng, X.; Sui, W.; Shu, C.; Wan, L. J. pH-Responsive Mechanism of a Deoxycholic Acid and Folate Comodified Chitosan Micelle under Cancerous Environment. *J. Phys. Chem. B* **2013**, *117*, 1261−1268.

(4) Yue, Z. G.; Wei, W.; You, Z. X.; Yang, Q. Z.; Yue, H.; Su, Z. G.; Ma, G. H. Iron Oxide Nanotubes for Magnetically Guided Delivery and pH-Activated Release of Insoluble Anticancer Drugs. *Adv. Funct. Mater.* **2011**, *21*, 3446−3453.

(5) Wang, H. J.; Cao, Y.; Cao, C.; Sun, Y. Y.; Yu, X. H.; Zhu, L. F.; Yang, L. Parinaric Acid Methyl Ester Polymer Films with Hill-Structured Features: Fabrication and Different Sensitivities to Normal and Tumor Cells. *ACS Appl. Mater. Interfaces* **2011**, *3*, 2755−2763.

(6) Wuang, S. C.; Neoh, K. G.; Kang, E. T.; Leckband, D. E.; Pack, D. W. Acid-Sensitive Magnetic Nanoparticles as Potential Drug Depots. *AIChE J.* **2011**, *57*, 1638−1645.

(7) Zhang, Z.; Chen, X.; Chen, L.; Yu, S.; Cao, Y.; He, C.; Chen, X. Intracellular pH-Sensitive PEG-Block-Acetalated-Dextrans as Efficient Drug Delivery Platforms. *ACS Appl. Mater. Interfaces* **2013**, *5*, 10760−10766.

(8) Yang, Y. Q.; Lin, W. J.; Zhao, B.; Wen, X. F.; Guo, X. D.; Zhang, L. J. Synthesis and Physicochemical Characterization of Amphiphilic

Triblock Copolymer Brush Containing pH-Sensitive Linkage for Oral Drug Delivery. *Langmuir* **2012**, *28*, 8251−8259.
(9) Giacomelli, F. C.; Stepánek, P.; Giacomelli, C.; Schmidt, V.; Jäger, E.; Jäger, A.; Ulbrich, K. pH-Triggered Block Copolymer Micelles Based on a pH-Responsive PDPA (Poly [2-(diisopropylamino) ethyl methacrylate]) Inner Core and a PEO (Poly (ethylene oxide)) Outer Shell as a Potential Tool for the Cancer Therapy. *Soft Matter* **2011**, *7*, 9316−9325.
(10) Sahoo, B.; Devi, K. S.; Banerjee, R.; Maiti, T. K.; Pramanik, P.; Dhara, D. Thermal and pH Responsive Polymer-Tethered Multifunctional Magnetic Nanoparticles for Targeted Delivery of Anticancer Drug. *ACS Appl. Mater. Interfaces* **2013**, *5*, 3884−3893.
(11) Huang, X.; Xiao, Y.; Lang, M. Synthesis and Self-Assembly Behavior of Six-Armed Block Copolymers with pH-and Thermo-Responsive Properties. *Macromol. Res.* **2011**, *19*, 113−121.
(12) Chen, J.; Qiu, X.; Ouyang, J.; Kong, J.; Zhong, W.; Xing, M. M. pH and Reduction Dual-Sensitive Copolymeric Micelles for Intracellular Doxorubicin Delivery. *Biomacromolecules* **2011**, *12*, 3601−3611.
(13) Oh, K. T.; Oh, Y. T.; Oh, N. M.; Kim, K.; Lee, D. H.; Lee, E. S. A Smart Flower-Like Polymeric Micelle for pH-Triggered Anticancer Drug Release. *Int. J. Pharmaceut.* **2009**, *375*, 163−169.
(14) Yoo, N. Y.; Youn, Y. S.; Oh, N. M.; Oh, K. T.; Lee, D. K.; Cha, K. H.; Oh, Y. T.; Lee, E. S. Antioxidant Encapsulated Porous Poly (lactide-*co*-glycolide) Microparticles for Developing Long Acting Inhalation System. *Colloid. Surface. B* **2011**, *88*, 419−424.
(15) Groot, R. D.; Warren, P. B. Dissipative Particle Dynamics: Bridging the Gap between Atomistic and Mesoscopic Simulation. *J. Chem. Phys.* **1997**, *107*, 4423−4435.
(16) Yan, L. T.; Zhang, X. Dissipative Particle Dynamics Simulations of Complexes Comprised of Cylindrical Polyelectrolyte Brushes and Oppositely Charged Linear Polyelectrolytes. *Langmuir* **2009**, *25*, 3808−3813.
(17) Wang, H.; Liu, Y. T.; Qian, H. J.; Lu, Z. Y. Dissipative Particle Dynamics Simulation Study on Complex Structure Transitions of Vesicles Formed by Comb-Like Block Copolymers. *Polymer* **2011**, *52*, 2094−2101.
(18) Gavrilov, A. A.; Kudryavtsev, Y. V.; Khalatur, P. G.; Chertovich, A. V. Microphase Separation in Regular and Random Copolymer Melts by DPD Simulations. *Chem. Phys. Lett.* **2011**, *503*, 277−282.
(19) Grafmüller, A.; Shillcock, J.; Lipowsky, R. The Fusion of Membranes and Vesicles: Pathway and Energy Barriers from Dissipative Particle Dynamics. *Biophys. J.* **2009**, *96*, 2658−2675.
(20) Srinivas, G.; Discher, D. E.; Klein, M. L. Self-Assembly and Properties of Diblock Copolymers by Coarse-Grain Molecular Dynamics. *Nat. Mater.* **2004**, *3*, 638−644.
(21) Loverde, S. M.; Klein, M. L.; Discher, D. E. Nanoparticle Shape Improves Delivery: Rational Coarse Grain Molecular Dynamics (rCG-MD) of Taxol in Worm-Like PEG-PCL Micelles. *Adv. Mater.* **2011**, *24*, 3823−3830.
(22) Hoogerbrugge, P.; Koelman, J. Simulating Microscopic Hydrodynamic Phenomena with Dissipative Particle Dynamics. *EPL-Europhys. Lett.* **1992**, *19*, 155−160.
(23) Español, P.; Warren, P. Statistical Mechanics of Dissipative Pparticle Dynamics. *EPL-Europhys. Lett.* **1995**, *30*, 191−196.
(24) Sheng, Y. J.; Nung, C. H.; Tsao, H. K. Morphologies of Star-Block Copolymers in Dilute Solutions. *J. Phys. Chem. B* **2006**, *110*, 21643−21650.
(25) Soto-Figueroa, C.; Vicente, L.; Martínez-Magadán, J. M.; Rodríguez-Hidalgo, M. D. R. Self-Organization Process of Ordered Structures in Linear and Star Poly (styrene)-Poly (isoprene) Block Copolymers: Gaussian Models and Mesoscopic Parameters of Polymeric Systems. *J. Phys. Chem. B* **2007**, *111*, 11756−11764.
(26) Guo, X. D.; Zhang, L. J.; Chen, Y.; Qian, Y. Core/Shell pH-Sensitive Micelles Self-Assembled from Cholesterol Conjugated Oligopeptides for Anticancer Drug Delivery. *AIChE J.* **2010**, *56*, 1922−1931.
(27) Xu, M. Y.; Yang, Z. R. Dissipative Particle Dynamics Study on the Mesostructures of n-Octadecane/Water Emulsion with Alternating Styrene-Maleic Acid Copolymers as Emulsifier. *Soft Matter* **2012**, *8*, 375−384.
(28) Arai, N.; Yasuoka, K.; Zeng, X. C. A Vesicle Cell under Collision with a Janus or Homogeneous Nanoparticle: Translocation Dynamics and Late-Stage Morphology. *Nanoscale* **2013**, *5*, 9089−9100.
(29) Groot, R. D.; Madden, T. J. Dynamic Simulation of Diblock Copolymer Microphase Separation. *J. Chem. Phys.* **1998**, *108*, 8713−8724.
(30) Groot, R. D.; Madden, T. J.; Tildesley, D. J. On the Role of Hydrodynamic Interactions in Block Copolymer Microphase Separation. *J. Chem. Phys.* **1999**, *110*, 9739−9749.
(31) Srinivas, G.; Mohan, R. V.; Kelkar, A. D. Polymer Micelle Assisted Transport and Delivery of Model Hydrophilic Components inside a Biological Lipid Vesicle: A Coarse-Grain Simulation Study. *J. Phys. Chem. B* **2013**, *117*, 12095−12104.
(32) Yang, C.; Sun, Y.; Zhang, L. Dissipative Particle Dynamics Study on Aggregation of MPEG-PAE-PLA Block Polymer Micelles Loading Doxorubicine. *Chin. J. Chem.* **2012**, *30*, 1980−1986.
(33) Ding, H. M.; Ma, Y. Q. Interactions between Janus Particles and Membranes. *Nanoscale* **2012**, *4*, 1116−1122.
(34) Liu, H.; Li, Y.; Krause, W. E.; Pasquinelli, M. A.; Rojas, O. J. Mesoscopic Simulations of the Phase Behavior of Aqueous $EO_{19}PO_{29}EO_{19}$ Solutions Confined and Sheared by Hydrophobic and Hydrophilic Surfaces. *ACS Appl. Mater. Interfaces* **2012**, *4*, 87−95.
(35) Rodríguez-Hidalgo, M. D. R.; Soto-Figueroa, C.; Vicente, L. Mesoscopic Simulation of the Drug Release Mechanism on the Polymeric Vehicle P (ST-DVB) in an Acid Environment. *Soft Matter* **2011**, *7*, 8224−8230.
(36) Guo, X. D.; Qian, Y.; Zhang, C. Y.; Nie, S. Y.; Zhang, L. J. Can Drug Molecules Diffuse into the Core of Micelles? *Soft Matter* **2012**, *8*, 9989−9995.
(37) Torchilin, V. P. Structure and Design of Polymeric Surfactant-Based Drug Delivery Systems. *J. Controlled Release* **2001**, *73*, 137−172.
(38) Ke, B. B.; Wan, L. S.; Zhang, W. X.; Xu, Z. K. Controlled Synthesis of Linear and Comb-Like Glycopolymers for Preparation of Honeycomb-Patterned Films. *Polymer* **2010**, *51*, 2168−2176.
(39) Pillai, O.; Panchagnula, R. Polymers in Drug Delivery. *Curr. Opin. Chem. Biol.* **2001**, *5*, 447−451.
(40) Yang, Y. Q.; Lin, W. J.; Zhang, L. J.; Cai, C. Z.; Jiang, W.; Guo, X. D.; Qian, Y. Synthesis, Characterization and pH-Responsive Self-Assembly Behavior of Amphiphilic Multiarm Star Triblock Copolymers Based on PCL, PDEAEMA, and PEG. *Macromol. Res.* **2013**, *21*, 1011−1020.
(41) Lin, Y. L.; Jiang, G.; Birrell, L. K.; El-Sayed, M. E. Degradable, pH-Sensitive, Membrane-Destabilizing, Comb-Like Polymers for Intracellular Delivery of Nucleic acids. *Biomaterials* **2010**, *31*, 7150−7166.
(42) Xiao, M.; Xia, G.; Wang, R.; Xie, D. Controlling the Self-Assembly Pathways of Amphiphilic Block Copolymers into Vesicles. *Soft Matter* **2012**, *8*, 7865−7874.
(43) Huang, J.; Wang, Y.; Laradji, M. Flow Control by Smart Nanofluidic Channels: a Dissipative Particle Dynamics Simulation. *Macromolecules* **2006**, *39*, 5546−5554.
(44) Li, X.; Pivkin, I. V.; Liang, H.; Karniadakis, G. E. Shape Transformations of Membrane Vesicles from Amphiphilic Triblock Copolymers: A Dissipative Particle Dynamics Simulation Study. *Macromolecules* **2009**, *42*, 3195−3200.
(45) Yue, T.; Wang, X.; Huang, F.; Zhang, X. An Unusual Pathway for the Membrane Wrapping of Rodlike Nanoparticles and the Orientation- and Membrane Wrapping-Dependent Nanoparticle Interaction. *Nanoscale* **2013**, *5*, 9888−9896.
(46) Xin, J.; Liu, D.; Zhong, C. Multicompartment Micelles from Star and Linear Triblock Copolymer Blends. *J. Phys. Chem. B* **2007**, *111*, 13675−13682.
(47) Guo, X. D.; Zhang, L. J.; Wu, Z. M.; Qian, Y. Dissipative Particle Dynamics Studies on Microstructure of pH-Sensitive Micelles for Sustained Drug Delivery. *Macromolecules* **2010**, *43*, 7839−7844.
(48) Kang, S.; Choi, I.; Lee, K. B.; Kim, Y. Bioconjugation of Poly(poly(ethylene glycol) methacrylate)-Coated Iron Oxide Mag-

netic Nanoparticles for Magnetic Capture of Target Proteins. *Macromol. Res.* **2009**, *17*, 259−264.
(49) Hu, F.; Neoh, K. G.; Kang, E. T. Synthesis of Folic Acid Functionalized PLLA-*b*-PPEGMA Nanoparticles for Cancer Cell Targeting. *Macromol. Rapid Commun.* **2009**, *30*, 609−614.
(50) Wang, Y.; Li, B.; Zhou, Y.; Lu, Z.; Yan, D. Dissipative Particle Dynamics Simulation Study on the Mechanisms of Self-Assembly of Large Multimolecular Micelles from Amphiphilic Dendritic Multiarm Copolymers. *Soft Matter* **2013**, *9*, 3293−3304.
(51) Nie, S. Y.; Sun, Y.; Lin, W. J.; Wu, W. S.; Guo, X. D.; Qian, Y.; Zhang, L. J. Dissipative Particle Dynamics Studies of Doxorubicin-Loaded Micelles Assembled from Four-Arm Star Triblock Polymers 4AS-PCL-*b*-PDEAEMA-*b*-PPEGMA and their pH-Release Mechanism. *J. Phys. Chem. B* **2013**, *117*, 13688−13697.
(52) Chen, H. Y.; Ruckenstein, E. Nanoparticle Aggregation in the Presence of a Block Copolymer. *J. Chem. Phys.* **2009**, *131*, 244904.
(53) Chen, H. Y.; Ruckenstein, E. Formation and Degradation of Multicomponent Multicore Micelles: Insights from Dissipative Particle Dynamics Simulations. *Langmuir* **2013**, *29*, 5428−5434.